Ocean stagnation and end-Permian anoxia

Roberta M. Hotinski* Department of Geosciences, Pennsylvania State University, University Park, Pennsylvania 16802, USA
Karen L. Bice Department of Geology and Geophysics, Woods Hole Oceanographic Institution, Woods Hole, Massachusetts 02543, USA
Lee R. Kump Department of Geosciences, Pennsylvania State University, University Park, Pennsylvania 16802, USA
Raymond G. Najjar Department of Meteorology, Pennsylvania State University, University Park, Pennsylvania 16802, USA
Michael A. Arthur Department of Geosciences, Pennsylvania State University, University Park, Pennsylvania 16802, USA

ABSTRACT

Ocean stagnation has been invoked to explain the widespread occurrence of organic-carbon–rich, laminated sediments interpreted to have been deposited under anoxic bottom waters at the time of the end-Permian mass extinction. However, to a first approximation, stagnation would severely reduce the upwelling supply of nutrients to the photic zone, reducing productivity. Moreover, it is not obvious that ocean stagnation can be achieved. Numerical experiments performed with a three-dimensional global ocean model linked to a biogeochemical model of phosphate and oxygen cycling indicate that a low equator to pole temperature gradient could have produced weak oceanic circulation and widespread anoxia in the Late Permian ocean. We find that polar warming and tropical cooling of sea-surface temperatures cause anoxia throughout the deep ocean as a result of both lower dissolved oxygen in bottom source waters and increased nutrient utilization. Buildup of quantities of H_2S and CO_2 in the Late Permian ocean sufficient to directly cause a mass extinction, however, would have required large increases in the oceanic nutrient inventory.

Keywords: Permian, anoxia, ocean circulation, phosphate cycle, oxygen cycle.

INTRODUCTION

A number of authors have proposed that sluggish or stagnant ocean circulation contributed to anoxia and the creation of large chemical gradients in ancient oceans (e.g., Fischer and Arthur, 1977; Bralower and Thierstein, 1984; Holser and Magaritz, 1987; Malkowski et al., 1989; Gruszczynski et al., 1992; Kajiwara et al., 1994; Isozaki, 1997). Geochemical evidence suggests that the Permian-Triassic boundary interval was such a period. Studies of boundary interval sediments reveal large negative excursions in carbon, sulfur, and strontium isotopic compositions of surface waters, which have been interpreted as evidence of chemically distinct deep waters upwelling into a previously isolated surface ocean (Holser and Magaritz, 1987; Gruszczynski et al., 1992; Malkowski et al., 1994; Kajiwara et al., 1994; Knoll et al., 1996). In addition, widespread laminated, pyritic sediments in Upper Permian and Lower Triassic sections (Wignall and Hallam, 1992, 1993; Wignall and Twitchett, 1996; Isozaki, 1997) suggest that, unlike today, decomposition of organic matter exhausted oxygen supplied by circulation throughout much of the water column. The magnitude and global nature of the excursions and anoxia led these investigators to propose that the entire ocean was severely stratified prior to the boundary, and that stagnation-induced anoxia may have played a role in the end-Permian extinction.

A potential flaw in this hypothesis is neglect of the relationship between ocean circulation and surface productivity. While ocean mixing acts to destroy vertical gradients in oxygen and other chemical species, it also returns nutrients to the surface that fuel the biological activity and organic-matter decomposition required to sustain gradients. Quantifying the results of this competition between circulation and biology thus requires a model that accounts for both ocean physics and a dynamic link between nutrients and productivity. Although Permian ocean circulation has been studied quantitatively in the past (Kutzbach et al., 1990), this is the first attempt to treat the Permian ocean's biogeochemistry explicitly.

We simulate a stagnation scenario for the Late Permian ocean using a three-dimensional ocean general circulation model that includes a simple biogeochemical model of phosphate and oxygen cycling. To assess whether ocean stagnation would have created the chemical patterns postulated for this time period, we apply a low equator-to-pole temperature gradient and examine the changes in circulation and chemical structure of the ocean that result.

MODEL DESCRIPTION

The general circulation model (GCM) used to simulate Permian ocean circulation is the Geophysical Fluid Dynamics Laboratory's Modular Ocean Model (MOM) (Pacanowski et al., 1993). The model configuration used includes $4° \times 4°$ resolution, 16 vertical levels, and constant vertical and horizontal mixing coefficients (1 cm^2/s and 2×10^7 cm^2/s, respectively). The ocean model bathymetry is a simplified flat-bottom case (5150 m depth) with continental boundaries that approximate the land and sea distribution in the Late Permian (Wordian) paleogeographical reconstruction of Rees et al. (1999). Further details of the model, including additional simulations and model limitations, can be obtained elsewhere.[1]

For this study, the MOM code was modified to include simple ocean biogeochemistry. Export of organic matter from the euphotic zone (100 m thick) is modeled using the relationship of Yamanaka and Tajika (1996). The export flux is proportional to surface-water phosphate concentration and varies with the cosine of latitude to simulate light limitation with increasing latitude. Phosphate, rather than nitrate, was chosen as the driver of productivity because phosphate is thought to exert the primary control on marine primary production on long time scales (e.g., Tyrrell, 1999). The exported organic flux is instantaneously remineralized below the euphotic zone according to the power law of Martin et al. (1987). Any flux that reaches the lowest vertical layer of the ocean is remineralized, consistent with observations that only a small fraction of the flux reaching the sediments is buried.

We assume that organic-matter decomposition will proceed via denitrification and sulfate reduction after oxygen is depleted, and specify that the rate of phosphate remineralization is independent of oxygen concentration in our model. However, because we do not include nitrate and sulfate as tracers, such remineralization is represented by negative values of dissolved O_2. Although the biogeochemical model greatly simplifies the cycling of organic matter, it produces realistic distributions of phosphate and oxygen in the modern ocean (Yamanaka and Tajika, 1996).

To examine the effects of a reduced latitudinal temperature gra-

*Present address: Atmospheric and Ocean Sciences Program, Princeton University, Princeton, New Jersey 08544, USA. E-mail: hotinski@princeton.edu.

[1]GSA Data Repository item 20016, Additional model description and parameters, is available on request from Documents Secretary, GSA, P.O. Box 9140, Boulder, CO 80301, editing@geosociety.org or at www.geosociety.org/pubs/ft2001.htm.

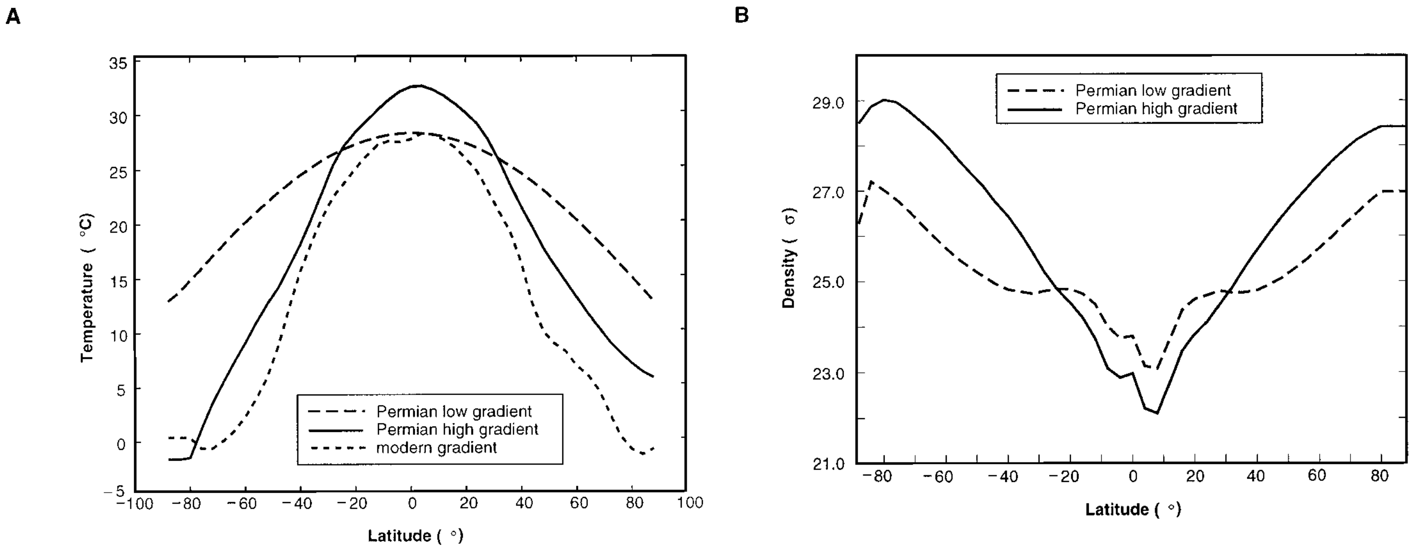

Figure 1. Model meridional (A) sea-surface temperature gradients and (B) surface density gradients for modern (A only), Permian high-gradient, and Permian reduced-gradient scenarios.

dient on the Permian ocean, the model was run with two sets of climatic forcings. A high-gradient forcing case used zonally averaged, mean annual temperature, salinity, and wind forcings predicted by a GENESIS version 2 simulation for the Late Permian (Wordian) that included Late Permian paleogeography, 2760 ppm CO_2 (about eight times the present atmospheric concentration), and 97.9% of the modern solar luminosity (Rees et al., 1999). The temperature gradient predicted by this simulation (Fig. 1A) is similar to the modern zonal average gradient. The ocean model was run for 2700 yr with the high-gradient forcing until a vigorous circulation was established.

To simulate climatic warming, the ocean model run was continued with the same wind-stress and salinity forcing boundary conditions as in the high-gradient case, but a new lower temperature gradient was applied. Sea-surface temperatures (SSTs) for this simulation were fixed at an equator-to-pole gradient of 12–28 °C (Fig. 1A), modeled after that of the Paleocene-Eocene boundary interval (Zachos et al., 1994; Bice et al., 2000). This gradient causes a substantial reduction in the ocean's pole to equator surface density gradient (Fig. 1B). Paleoclimatological evidence (Taylor et al., 1992) suggests that the Late Permian southern polar climate was comparable to Paleocene-Eocene Arctic climate, temperatures being >10 °C for at least a third of the year (Ziegler, 1990; Yemane, 1993). In addition, oxygen isotope and paleosol data indicate warming from the latest Permian into the earliest Triassic (Holser et al., 1991; Retallack, 1999).

RESULTS

Circulation

The steady-state meridional overturning (zonally integrated mass transport stream function in the meridional vertical plane) for the high-gradient scenario is shown in Figure 2A. The pattern is asymmetrical; there is a strong cell in the Southern Hemisphere and a weaker cell in the Northern Hemisphere. The maximum Southern Hemisphere transport value is >80 Sverdrups (1 Sv $= 1 \times 10^6$ m^3 s^{-1}) and the circulation can be characterized as vigorous.

This vigorous circulation is disrupted when the reduced temperature gradient is applied (Fig. 2). At 100 yr, the ocean is poorly mixed and is dominated below 1000 m by Northern Hemisphere sinking. By 1200 yr, weak mixing between the surface and deep ocean is reestablished. After 10 k.y., circulation has reached a new steady state with substantially reduced overturning relative to the high-gradient case, consistent with the reduction in upper ocean density between the simulations. The steady state thermohaline circulation, driven by a weaker, but largely symmetrical, density contrast (Fig. 1B), exhibits much less interhemispheric asymmetry than the high-gradient circulation (Fig. 1A). Although circulation is reduced, bottom water is still formed at high latitudes in both hemispheres and there is no low-latitude deep-water formation. Northern Hemisphere deep waters are ventilated at a rate nearly comparable to that of modern North Atlantic Deep Water, estimated to be ~20 Sv (Broecker, 1991).

Dissolved Oxygen

The high-gradient case is characterized by high values of dissolved O_2 in the high latitudes and in deep water (Fig. 3). The ocean is oxic everywhere except in intermediate waters off the western coast of Pangea (Fig. 3A), where negative values of O_2 indicate oxidation of organic matter with electron acceptors other than oxygen (i.e., nitrate and sulfate). The deep ocean is particularly well oxygenated (Fig. 3B); minimum O_2 values are >150 μmol/L. In comparison, modern North Pacific deep waters average ~130 μmol/L.

When the ocean reaches a steady state after application of the reduced temperature gradient, oxygen concentrations below the top 100 m are reduced by an average of 264 μmol/L. Deep ocean oxygen levels are dysoxic (<45 μmol/L) to anoxic over a majority of the deep-sea floor (Fig. 3D), and intermediate water oxygen concentrations are negative; values are as low as −300 μmol/L off the western coast of the supercontinent (Fig. 3C).

Knoll et al. (1996) discussed a box model of Permian anoxia and suggested that utilization of ~470 μmol/L of sulfate in the Late Permian caused buildup of lethal CO_2 levels in the deep ocean and contributed to the end-Permian extinction. Because sulfate has twice the reducing power of oxygen, this amount of sulfate reduction would correspond to values of ~−1000 μmol/L oxygen in the model. Such levels are not even approached in the reduced-gradient simulation. Therefore, some factor in addition to reduced overturning seems necessary to create such high levels of CO_2 in the Late Permian deep ocean.

DISCUSSION AND CONCLUSIONS

Our results suggest that deep-ocean anoxia is consistent with reduced thermohaline circulation driven by a low meridional density contrast. However, almost half the difference between the simulated high-gradient and reduced-gradient deep water oxygen levels is due to the difference in solubility of oxygen in the warmed high-latitude regions where deep waters are formed (~250 μmol/L, vs. 370 μmol/L in the

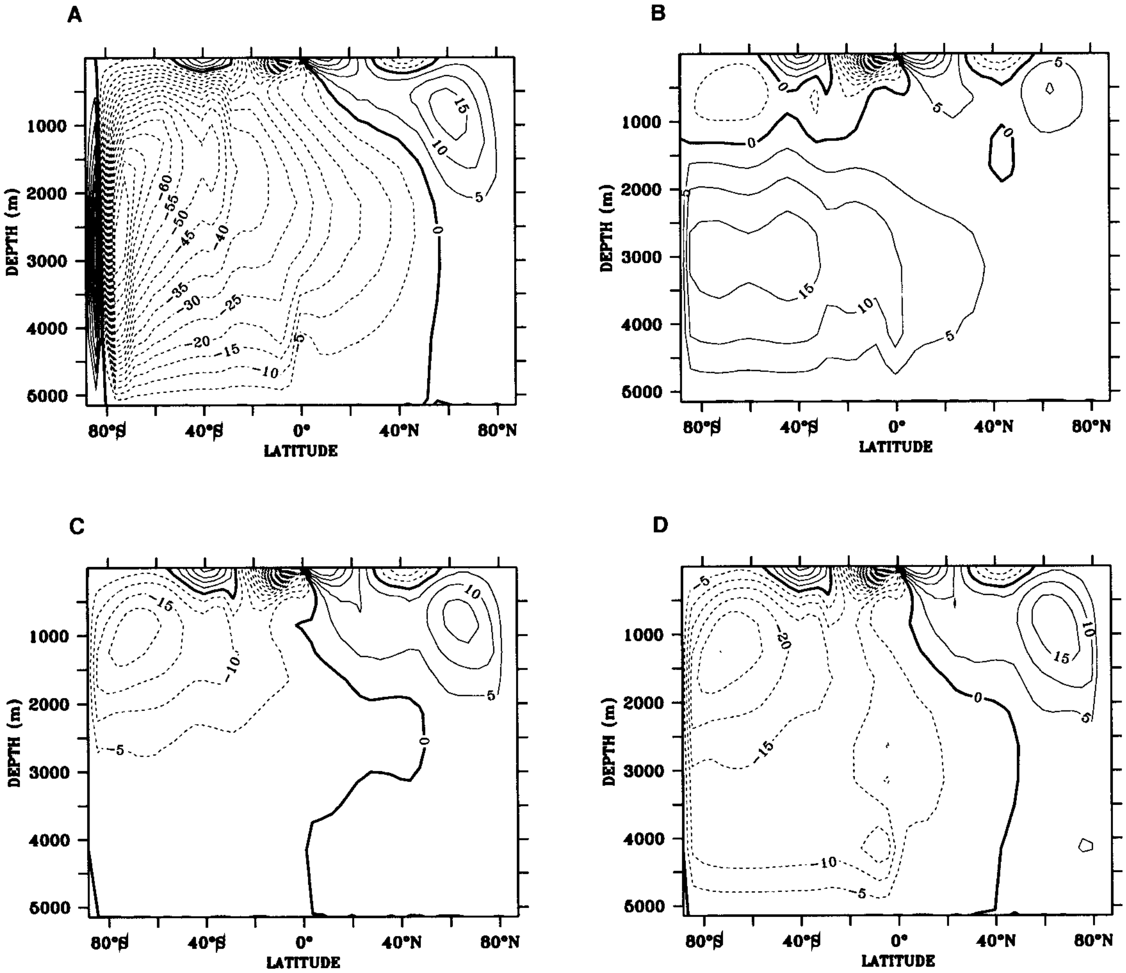

Figure 2. Simulated meridional overturning (zonally integrated volume transport stream function in meridional vertical plane) for Permian ocean in Sverdrups (Sv; 10^6 m^3/s). Positive values indicate clockwise flow, and negative values indicate counterclockwise flow. Modular ocean model (MOM) (A) equilibrated with high-gradient sea-surface temperature forcing, and (B) 100 yr, (C) 1200 yr, and (D) 10 k.y. after imposing reduced-gradient forcing.

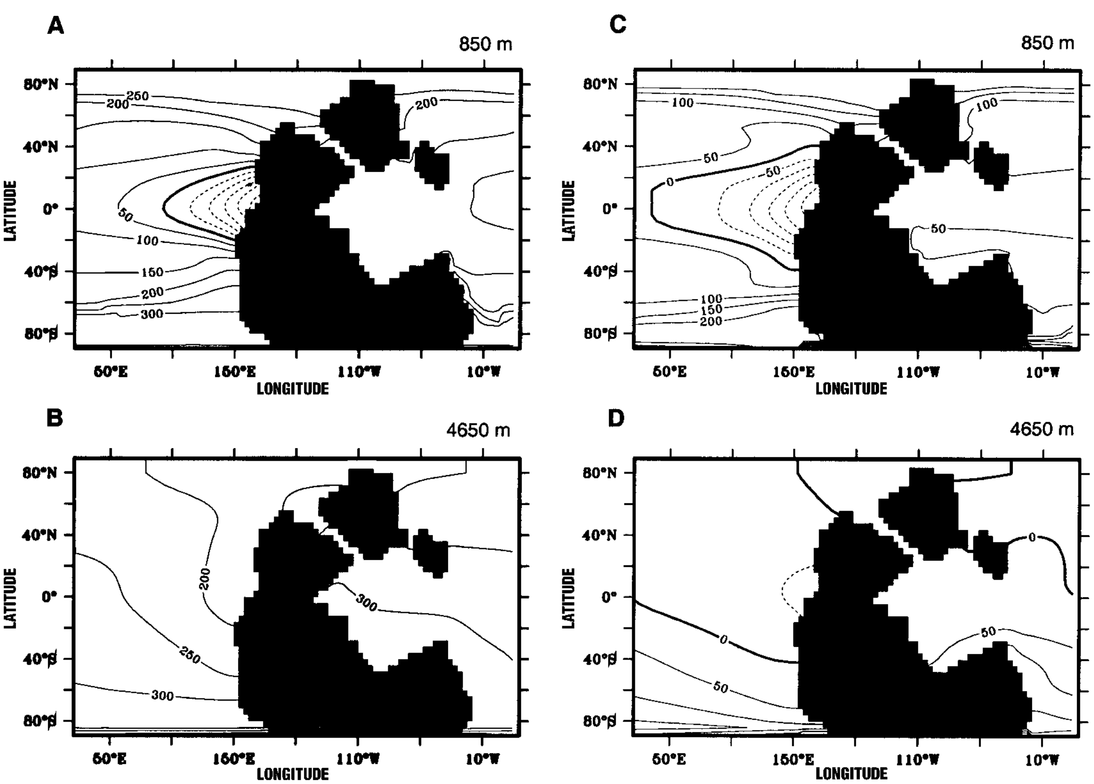

Figure 3. Maps of steady-state oxygen concentrations (μmol/L) for (A) intermediate (850 m) and (B) deep ocean (4650 m) in high-gradient scenario; (C) upper intermediate and (D) deep ocean in reduced-gradient scenario.

high-gradient scenario). This result is consistent with box modeling results for the Cretaceous (Herbert and Sarmiento, 1991). Biological oxygen demand explains the remainder of the oxygen decline ($\sim$140 μmol/L), but the magnitude of this oxygen demand alone would not drive the reduced-gradient ocean completely anoxic without the aforementioned temperature effect. Chemical stratification is limited because decreased upwelling rates of nutrients in the reduced-gradient case support lower export of organic matter from surface waters than in the high-gradient case (14.3 vs. 19.8 Gt C/yr). The effects of slowed ventilation and dwindling productivity do not exactly balance because the surface biota exploit a reserve source of nutrients, i.e., high-latitude phosphate.

Because of light limitation at high latitudes, the high-gradient scenario with vigorous upwelling exhibits phosphate concentrations $>$2 μmol/L in southern high latitudes and 1.5 μmol/L in the northern areas of convection. In the reduced-gradient scenario, with slower upwelling and longer high-latitude surface-water residence times, phosphate values in surface waters of both the northern and southern high latitudes decline by $\sim$0.4 and 0.8 μmol/L, respectively (not shown). As a result, 3.62×10^{20} mol of phosphate are lost from surface waters in the reduced-gradient case, fueling export of organic matter that drives already low deep-water oxygen concentrations to anoxic levels. This sensitivity of deep-water oxygenation to high-latitude productivity is consistent with the box-modeling results of Sarmiento et al. (1988) and Hotinski et al. (2000). Thus, although the reduced-gradient scenario exhibits widespread anoxia, relatively high rates of ventilation and reduced productivity keep the deep ocean near the oxic-anoxic boundary, rather than firmly in the regime of sulfate reduction. Increasing the marine phosphate inventory by 50% increases chemical stratification in the model (results not shown), but five times more phosphate would be needed to drive the system to the values suggested by Knoll et al. (1996). Because the phosphate content of the Permian ocean is not well determined, such a high value cannot be ruled out (Martin, 1995). High steady-state phosphate concentrations in pore waters of modern marine sediments, which commonly approach 10 μmol/L, indicate that high levels of phosphate are sustainable (Emerson et al., 1980; Van Cappellen and Berner, 1988). Thus, it is possible that the Permian ocean's phosphate concentration was significantly higher than today's value of 2.15 μmol/L.

ACKNOWLEDGMENTS

Financial support was provided by the NASA Astrobiology Institute Cooperative Agreement (NCC2-1057), the National Science Foundation (grant EAR-98-05139), the Shell Oil Company Foundation, and the Pennsylvania Space Grant Consortium. We thank Tim Bralower for a thoughtful review of the manuscript.

REFERENCES CITED

Bice, K.L., Sloan, L.C., and Barron, E.J., 2000, Comparison of early Eocene isotopic paleotemperatures and the three-dimensional OGCM temperature field: The potential for use of model-derived surface water δ^{18}O, *in* Huber, B.T., et al., eds., Warm climates in Earth history: Cambridge, UK, Cambridge University Press, p. 79–131.

Bralower, T.J., and Thierstein, H.R., 1984, Low productivity and slow deep-water circulation in mid-Cretaceous oceans: Geology, v. 12, p. 614–618.

Broecker, W.S., 1991, The great ocean conveyor: Oceanography, v. 4, p. 79–89.

Emerson, S., Jahnke, R., Bender, M., Froelich, P., Klinkhammer, G., Bowser, C., and Setlock, S., 1980, Early diagenesis in sediments from the eastern Equatorial Pacific, I. Pore water nutrient and carbonate results: Earth and Planetary Science Letters, v. 49, p. 57–80.

Fischer, A.G., and Arthur, M.A., 1977, Secular variations in the pelagic realm, *in* Cook, H.E., and Enos, P., eds., Deep-water carbonate environments: Society of Economic Paleontologists and Mineralogists Special Publication 25, p. 19–50.

Gruszczynski, M., Hoffman, A., Malkowski, K., and Veizer, J., 1992, Seawater strontium perturbation at the Permian-Triassic boundary, West Spitsbergen, and its implications for the interpretation of strontium isotopic data: Geology, v. 20, p. 779–782.

Herbert, G.D., and Sarmiento, J.L., 1991, Ocean nutrient distribution and oxygenation: Limits on the formation of warm saline bottom waters over the past 91 m.y.: Geology, v. 19, p. 702–705.

Holser, W.T., and Magaritz, M., 1987, Events near the Permian-Triassic boundary: Modern Geology, v. 11, p. 155–180.

Holser, W.T., Schönlaub, H.P., Boeckelman, K., and Magaritz, M., 1991, The Permian-Triassic of the Gartnerkofel-1 core (Carnic Alps, Austria): Synthesis and conclusions, *in* Holser, W.T., and Schönlaub, H.P., eds., The Permian-Triassic boundary in the Carnic Alps of Austria (Gartnerkofel region): Abhandlungen Geologische Bundesantstalt Austriche, v. 45, p. 213–232.

Hotinski, R.M., Kump, L.R., and Najjar, R.G., 2000, Opening Pandora's Box: The impact of open-system modeling on interpretations of anoxia: Paleoceanography, v. 15, p. 267–279.

Isozaki, Y., 1997, Permo-Triassic boundary superanoxia and stratified superocean: Records from lost deep-sea: Science, v. 276, p. 235–238.

Kajiwara, Y., Yamakita, S., Ishida, K., Ishiga, H., and Imai, A., 1994, Development of a largely anoxic stratified ocean and its temporary massive mixing at the Permian/Triassic boundary supported by the sulfur isotopic record: Palaeogeography, Palaeoclimatology, Palaeoecology, v. 111, p. 367–379.

Knoll, A.H., Bambach, R.K., Canfield, D.E., and Grotzinger, J.P., 1996, Comparative Earth history and Late Permian mass extinction: Science, v. 273, p. 452–457.

Kutzbach, J.E., Guetter, P.J., and Washington, W.M., 1990, Simulated circulation of an idealized ocean for Pangaean time: Paleoceanography, v. 5, p. 299–317.

Malkowski, K., Gruszczynski, M., Hoffman, A., and Halas, S., 1989, Oceanic stable isotopic composition and a scenario for the Permo-Triassic crisis: Historical Biology, v. 2, p. 289–309.

Martin, J.H., Knauer, G.A., Karl, D.M., and Broenkow, W.W., 1987, VERTEX: Carbon cycling in the northeast Pacific: Deep Sea Research, v. 32, p. 267–286.

Martin, R.E., 1995, Cyclic and secular variation in microfossil mineralization, clues to the biogeochemical evolution of Phanerozoic oceans: Global and Planetary Change, v. 11, p. 1–23.

Pacanowski, R., Dixon, K., and Rosati, A., 1993, The Geophysical Fluid Dynamics Laboratory modular ocean users guide: Geophysical Fluid Dynamics Laboratory Ocean Group Technical Report 2.

Rees, P.M., Gibbs, M.T., Ziegler, A.M., Kutzbach, J.E., and Behling, P.J., 1999, Permian climates; evaluating model predictions using global paleobotanical data: Geology, v. 27, p. 891–894.

Retallack, G., 1999, Postapocalyptic greenhouse paleoclimate revealed by earliest Triassic paleosols in the Sydney Basin, Australia: Geological Society of America Bulletin, v. 111, p. 52–70.

Sarmiento, J.L., Herbert, T.D., and Toggweiler, J.R., 1988, Causes of anoxia in the world ocean: Global Biogeochemical Cycles, v. 7, p. 417–450.

Taylor, E.L., Taylor, T.N., and Cúneo, N.R., 1992, The present is not the key to the past: A polar forest from the Permian of Antarctica: Science, v. 257, p. 1675–1677.

Tyrrell, T., 1999, The relative influences of nitrogen and phosphorus on oceanic primary production: Nature, v. 400, p. 525–531.

Van Cappellen, P., and Berner, R.A., 1988, A mathematical model for the early diagenesis of phosphorus and fluorine in marine sediments: Apatite precipitation: American Journal of Science, v. 288, p. 289–333.

Wignall, P.B., and Hallam, A., 1992, Anoxia as a cause of the Permian/Triassic mass extinction, facies evidence from northern Italy and the western United States: Palaeogeography, Palaeoclimatology, Palaeoecology, v. 93, p. 21–46.

Wignall, P.B., and Hallam, A., 1993, Griesbachian (Early Triassic) palaeoenvironmental changes in the Salt Range, Pakistan and southeast China and their bearing on the Permo-Triassic extinction: Palaeogeogragraphy, Palaeoclimatology, Palaeoecology, v. 102, p. 215–237.

Wignall, P.B., and Twitchett, R.J., 1996, Oceanic anoxia and the end Permian mass extinction: Science, v. 272, p. 1155–1158.

Yamanaka, Y., and Tajika, E., 1996, The role of the vertical fluxes of particulate organic matter and calcite in the oceanic carbon cycle; studies using an ocean biogeochemical general circulation model: Global Biogeochemical Cycles, v. 10, p. 361–382.

Yemane, K., 1993, Contribution of Late Permian palaeogeography in maintaining a temperate climate in Gondwana: Nature, v. 361, p. 51–54.

Zachos, J.C., Stott, L., and Lohmann, K.C., 1994, Evolution of early Cenozoic marine temperatures: Paleoceanography, v. 9, p. 353–387.

Ziegler, A.M., 1990, Phytogeographic patterns and continental configurations during the Permian Period, *in* McKerrow, W.S., and Scotese, C.R., eds., Palaeozoic palaeogeography and biogeography and climatology: Geological Society [London] Memoir 12, p. 363–379.

Manuscript received May 1, 2000
Revised manuscript received September 21, 2000
Manuscript accepted October 4, 2000

Printed in USA